

Review Article

Cryo-EM in drug discovery

 **Tom Ceska¹, Chun-Wa Chung², Rob Cooke³, Chris Phillips⁴ and Pamela A. Williams⁵**

¹UCB Pharma, 216 Bath Road, Slough SL1 3WE, U.K.; ²GSK, GlaxoSmithKline R&D, Gunnelswood Road, Stevenage SG1 2NY, U.K.; ³Heptares Therapeutics Limited, Steinmetz Building, Granta Park, Great Abington, Cambridge CB21 6DG, U.K.; ⁴Discovery Sciences, IMED Biotech Unit, AstraZeneca, 310 Cambridge Science Park, Milton Road, Cambridge CB4 0WG, U.K.; ⁵Astex Pharmaceuticals, 436 Cambridge Science Park, Milton Road, Cambridge CB4 0QA, U.K.

Correspondence: Tom Ceska (tom.ceska@ucb.com)



The impact of structural biology on drug discovery is well documented, and the work-horse technique for the past 30 years or so has been X-ray crystallography. With the advent of several technological improvements, including direct electron detectors, automation, better microscope vacuums and lenses, phase plates and improvements in computing power enabled by GPUs, it is now possible to record and analyse images of protein structures containing high-resolution information. This review, from a pharmaceutical perspective, highlights some of the most relevant and interesting protein structures for the pharmaceutical industry and shows examples of how ligand-binding sites, membrane proteins, both big and small, pseudo symmetry and complexes are being addressed by this technique.

Introduction

The award of the 2017 Nobel Prize in Chemistry to Jacques Dubochet, Joachim Frank and Richard Henderson for developments in cryo-EM (cryo-electron microscopy) is perhaps proof, if needed, that cryo-EM is now a well-established tool for structure determination. The very nature of the technique, however, currently requires apparatus and facilities that only come with a significant investment, and thus, the barrier to evaluating cryo-EM within an industrial setting remains relatively high. There are many reasons why overcoming this barrier is desirable (the amount of protein sample required, the composition and molecular mass of the sample, be it single protein, complex or membrane-associated). The demand for high-end microscope time in academic research establishments outstrips availability, thus accessing and evaluating the technique via collaboration is somewhat limited. This led to discussions between a handful of interested pharmaceutical companies and FEI (now Thermo Fisher) in 2015, around the potential formation of a Cambridge Pharma EM consortium. FEI identified the Nanoscience Centre in the University as a suitable location for the instrument, and the MRC LMB agreed to provide support in sample preparation and initial data analysis, to help with the initial hurdle of making suitable grids and assessing their quality. Thus, there are five Pharma members (Astex, AstraZeneca, GlaxoSmithKline, Heptares and UCB), and two academic members (University of Cambridge and the MRC LMB) accessing a Krios microscope, which has been supported by FEI application scientists since 1 July 2016.

Protein structure is now routinely used in all parts of the drug discovery process, from the initial selection of protein to be targeted, the identification and optimisation of chemical hit matter against the target and the multi-threaded process by which the final properties of the compound are developed, leading to the final clinical candidate (Figure 1). In this context, a chemical hit is the first visualisation of a small molecule bound to the target protein. This has traditionally been done crystallographically by examining difference electron density maps. With the advent of high-resolution EM maps, small compounds can be visualised directly. Confirmation of binding is typically done by collecting data on close analogues, and this strategy could be employed with EM collected data. Binding modes are passed over for CADD analysis (Computer Aided Drug Design) for further compound elaboration to improve affinity and selectivity.

Received: 23 August 2018
 Revised: 5 December 2018
 Accepted: 6 December 2018

Version of Record published:
 15 January 2019

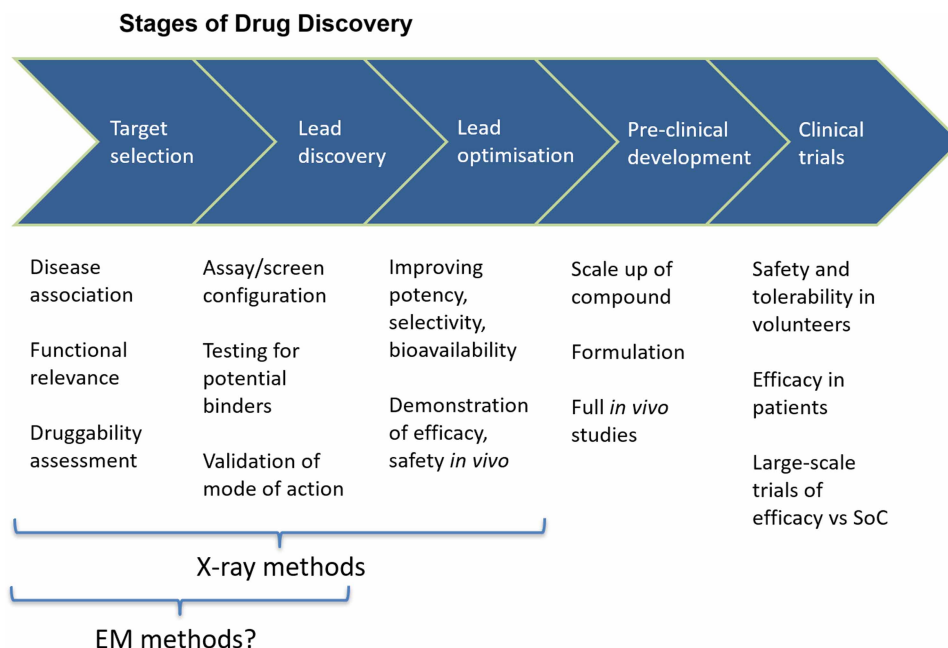


Figure 1. The drug discovery paradigm.

The conceptual pathway taken along the drug discovery pathway. X-ray crystallography is heavily used in the lead discovery and lead optimisation stages of a project. As the throughput of current cryo-EM methods is low, it is likely that binding of compounds at the initial stage of a project will make the most impact for NCE (New Chemical Entity) projects and Fab/antigen complexes to understand MOA for NBE (New Biological Entity) projects.

With the massive and continuing improvements in hardware and software involved in cryo-EM over the last few years, we can now evaluate the role of cryo-EM in providing an additional route to the structural information required to guide structure-based drug design, in addition to X-ray crystallography, NMR and homology modelling. The reported resolution of cryo-EM structures has historically been lower than X-ray crystallography-generated structures, but it is important to note the difference in how resolution is reported for the two techniques. As a result, the paradigm that higher than 2.5–3.0 Å resolution is required for structure-based drug discovery (based on crystal structures) may not hold for cryo-EM structures.

A recent review from Renaud et al. [1] surveyed the literature and described the state of the art cryo-EM process, as it stands now. Briefly, the method for sample preparation and analysis consists of applying a purified monodisperse protein sample onto an electron microscope grid, which acts as a support for the sample. The grids are manufactured to have a thin polymer layer with evenly spaced holes, and the protein molecules are suspended in these holes. The grid is flash frozen so the protein is trapped in vitreous ice. The evenly spaced holes make automated data collection possible. The protein molecules are ideally isolated from neighbouring molecules and in random orientations. Single-particle analysis using programmes such as Relion [2] extracts just the individual molecules from the images, centres each particle and averages the molecules, first in two dimensions and then in three dimensions to eventually give a 3D density map into which an atomic model can be built. The actual process is somewhat more complicated than described in this brief summary. The aim of this review is to sample selected publications illustrating how cryo-EM structures are starting to make an impact in a drug discovery setting.

Recent cryo-EM structures of drug discovery relevant proteins

Cryo-EM structures with ligands

It could be argued at which stage of the drug development pipeline, cryo-EM will have the greatest impact (Figure 1). For the moment with the current technology, it is like to be at the target identification and hit

identification phases, but further improvements could push the application into a cycle of lead optimisation as is the current practice using X-ray crystallography. There are as yet no published instances of a drug discovery campaign guided by cryo-EM, but there are many structures with small molecules bound which start to reveal the potential of cryo-EM in small-molecule drug discovery. The structure of β -galactosidase in complex with an inhibitor solved to a resolution of 2.2 Å in 2015 [3] was one of the first structures after the 'Resolution Revolution' announcement [4], and this resolution has recently been extended to 1.9 Å due to improvements in data processing [5]. The density allows placement of the ligand, water and ion molecules in the binding site, but perhaps more importantly highlights the fact that the cryo-EM data processing continues to evolve and that additional improvements should be expected. The structure of *Leishmania donovani* ribosome in complex with the antibiotic paromycin [6] has a reported overall resolution of 2.5 Å (extending to 2.2 Å at the core where the primary binding sites are). Paromycin targets the cytosolic ribosome of the *Leishmania* parasite, but has broad antimicrobial properties. The binding mode of the approved drug is consistent with mutational data generated by the project and provides a hypothesis for the development of additional compounds which may be more selective. The quality of the map also allowed the identification of ligands at secondary binding sites, peripheral from the core of the molecule. A summary of the protein structures discussed in this review is given in Table 1.

G protein-coupled receptors

While G protein-coupled receptors (GPCRs) represent the most common class of protein targets for therapeutic intervention, until relatively recently supporting drug discovery activities with structural and biophysical investigations was not feasible due to the instability of GPCRs when removed from the cell membrane. Over the past 10 years, developments in protein engineering and protein handling have led to X-ray crystal structures for more than 40 GPCRs, with consequent utility for drug discovery programmes. Crystallisation of GPCRs is still a major challenge, and the advent of single-particle cryo-EM as an alternative means of achieving atomic resolution structures has attracted considerable interest. Owing to the reasonably small size of GPCRs (the most common, Class A, are ~50 kDa), the initial focus has been on complexes with signalling partners, which, as well as providing direct views of the activated state of the receptor, have the added advantage of being a more suitable size for single-particle studies.

The first reported cryo-EM structure of a GPCR was for the calcitonin receptor [7], complexed with a high-affinity peptide agonist, and with the G_s protein assembly responsible for signal transmission from the activated receptor. The total size of the complex is ~150 kDa and a phase plate was used during data collection which improves the image contrast and can assist in structure determination for smaller proteins and complexes. Unlike the situation with GPCR crystal structures, the protein did not require engineering beyond the addition of tags for purification. The overall nominal resolution is 4.1 Å, but reaches 3.8 Å in the transmembrane and G protein regions. Comparison with crystal structures of inactive forms of Class B GPCRs revealed significant differences; as expected, the sixth transmembrane helix is moved away from the helical bundle on the intracellular side, to accommodate the G protein, but unexpectedly the extracellular end also moves outwards considerably to accommodate the peptide agonist. As this is a Class B receptor, a large extracellular domain (ECD) is present, but unfortunately is of lower resolution than the rest of the structure, with evidence for multiple orientations relative to the transmembrane region and hence, details of the interaction between the peptide agonist and the ECD are not resolvable. ECD domains of membrane proteins have been solved by X-ray crystallography [8], which could be used to improve the structural model. The binding site of the peptide with the transmembrane domain is visible, and is broader and shallower than previously envisaged, but the peptide in this region could not be unambiguously fitted to the cryo-EM data alone, requiring additional guidance based on mutagenesis experiments.

The cryo-EM structure of the Glp-1 receptor (GLP1R), also in complex with G protein and an agonist peptide, was reported soon after [9] (Figure 2). The particle size is similar to that of the calcitonin receptor, and again the overall nominal resolution is 4.1 Å, and slightly better in the transmembrane and G protein regions, but in this case a phase plate was not used during data collection. Although an inactive form of the GLP1R was not available for comparison, the authors inferred the structural changes upon activation by comparison with the inactive glucagon receptor. Activation by a peptide which bridges the extracellular and transmembrane domains is a common feature of Class B GPCRs, and mimicking this with a small-molecule therapeutic has been a long-desired ambition for many people, with a near total lack of success so far. Many hope that the structural insights now available may overcome this. Another structure of the GLP1R–G protein complex and a different agonist peptide was subsequently reported at 3.3 Å global resolution [10]. In addition

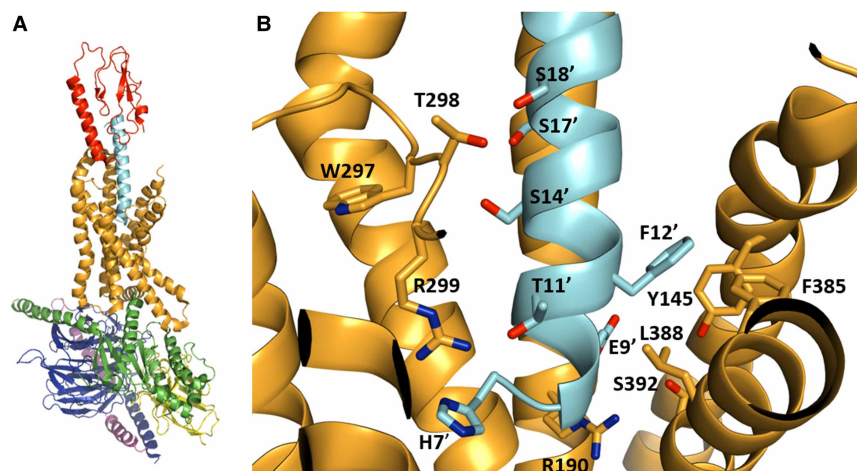


Figure 2. The Glp1R complex as reported by Zhang et al. [9] (pdb ref: 5vai).

(A) A cartoon plot of the assembly with Glp1 in pale blue, the ECD of Glp1R in red, the TM domain of Glp1R in gold, $G\alpha_s$ subunit in green, $G\beta$ subunit in dark blue, $G\gamma$ subunit in purple, and a stabilising nanobody in yellow. (B) A section of the structure with some of the residues of Glp1R and Glp1 highlighted by Zhang et al. as being important for binding and activation.

to giving a higher resolution view of the complex, several differences were observed which may contribute to the different profiles of activation between the peptides across multiple G proteins.

The structure of the adenosine A_{2A} receptor, bound to a differently engineered G protein complex and a small agonist, represents the first cryo-EM structure of a Class A GPCR [11]. The final global resolution is 4.1 Å, which in this case appears to be limited by conformational heterogeneity of the γ subunit of the G protein. Comparison with the crystal structure of an equivalent complex highlights flexibility within a loop on the extracellular surface of the cryo-EM structure and some different interactions with the G protein assembly. The cryo-EM structure was obtained at a more physiologically relevant pH and was not subject to crystal packing restraints; hence, the flexibility observed in the cryo-EM structure may be of more relevance for drug discovery.

Following the first four GPCR cryo-EM structures, which were obtained with various G_s assemblies, three recent examples have used different G proteins. The structure of the human adenosine A_1 receptor was determined at 3.6 Å resolution bound to adenosine and complexed with G_i [12]. While the data quality was sufficient to position adenosine in the receptor, and to allow comparison with the structure with two examples of inactive forms of the receptor, the emphasis was the comparison with the previously reported structures of G_s coupled receptors, and whether the determinants of G protein selectivity could be ascertained. Mindful of over-interpreting the data, the authors suggest differences in the tilt of helix 6 may be significant. Similarly, the emphasis on the report of the 3.8 Å structure of the serotonin 5HT_{1B} receptor coupled to G_0 [13] was not on the bound agonist Donatriptan, but on the interactions between the GPCR and the G protein. This study highlights the $\alpha 5$ helix of the $G_{\alpha 0}$ subunit and differences in the angle at which it sits in the GPCR. The interface between this GPCR and G_0 appears to be smaller than the interfaces with G_s , raising the possibility that the kinetics of dissociation of the G proteins may differ. The 3.5 Å structure of the mu opioid receptor complexed with G_i and DAMGO [14], a mimic of the natural peptide agonist, revealed that the key interactions between DAMGO and the receptor are similar to those of the constrained agonist BU72, but, unsurprisingly, DAMGO appears much more flexible, and molecular dynamics simulations were required to identify more interactions with the protein. While differences are apparent from G_s coupled receptors, the authors concede that a more comprehensive profiling of complexes will be required to fully understand the picture.

The emphasis of these studies has been on the mechanisms of GPCR activation and how selectivity for different G proteins is achieved. For many GPCRs, the profile of activation across G proteins, and between G proteins and arrestins, is an important consideration for a therapeutic agent. Interestingly, the investigators feel that their conclusions are not limited by the resolution of the structures, but more by not always having structures of the relevant forms. Doubtless more structures of GPCRs in complex with G proteins will emerge in the next few years, and the technology will hopefully develop to enable visualisation of inactive forms, in the

absence of G proteins, which are more relevant for some indications. Resolution of the structures will become a more important consideration as the emphasis shifts to interactions with ligands.

Ion channels

A major drive for the Pharma Industry's adoption of cryo-EM is the expansion of protein target classes for which structural information can drive project decisions, either through an improved mechanistic understanding of disease biology or through high-quality atomistic experimental models of ligand–protein complexes. Perhaps, the best example of this impact is the transient receptor potential (TRP) family of ion channels. In recent years, several near-atomic and atomic cryo-EM structures of TRP family members have not only advanced our understanding of the structural–functional relationships governing the molecular mechanism of this significant target class, but are informing ligand design and impacting medicinal chemistry programmes (see ref. [15] for review). Cryo-EM has many advantages over crystallography for the study of TRP channels. Firstly, making large amounts (multi mg) of homogeneous channel has proved challenging and cryo-EM, although still requiring high-quality protein, is less stringent in terms of protein quantity. Additionally, the use of nanodiscs, synthetic membrane discs [16], to stabilise the purified functional channel has been very successful in facilitating cryo-EM reconstructions.

The wealth of TRP channel structures not only allows for us to understand the general features of the family but also significantly to examine differences and understand both ion and ligand selectivity. TRP channels are grouped into six subfamilies: TRPA, TRPC, TRPM, TRPML, TRPP and TRPV, and cryo-EM structures have now been determined for members of all subfamilies. TRP channels are tetrameric and contain a conserved transmembrane domain made up of six membrane spanning helices from each monomer, four of these helices form a bundle which packs with the remaining two helices from an adjacent monomer, termed a 'domain swap' arrangement. The close homology across the subfamilies breaks down beyond the membrane, and numerous arrangements of ankyrin repeats are observed within the cytosolic region while some classes have large extracellular regions. As many as 48 cryo-EM structures of TRP channels were deposited between 2013 and 2017, with several being at resolutions better than 3 Å. The impact the first near-atomic resolution cryo-EM structures of a novel protein class is well demonstrated by the capsaicin (vanilloid) receptor TRPV1 structure published in 2013 [17,18] (Figure 3). These structures of ligand-free and -bound states provide a mechanistic basis for channel opening on ligand activation and detail the conformational dynamics controlling ion permeation and channel gating. Densities for the small-molecule agonists resiniferatoxin and capsaicin were resolved. A higher resolution structure of the capsaicin-bound form [19] allowed the small-molecule-bound complex to be modelled. Additionally, the same team has provided ligand-bound structures of the TRPA1 channel with both agonist and antagonists bound [20] identifying a novel pharmacological site.

Reports of the use of these TRP channel cryo-EM structures in a traditional structure-based drug design 'hit-to-lead' setting are beginning to emerge. The structure of a high-affinity ligand, termed BTDM, to the novel TRPC6 channel structure, a target for certain kidney diseases, has recently been described [21]. The inhibitor binds between the helix bundle of one subunit and the fifth and sixth transmembrane helices of the adjacent subunit preventing channel opening, in a position similar to the site observed for RTX and capsaicin on TRPV1 [17].

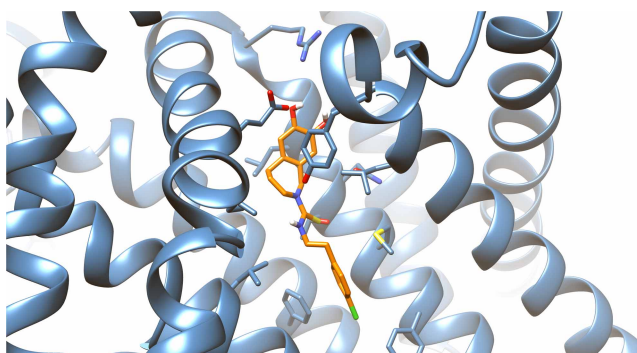


Figure 3. TRPV1 channel.

Small-molecule-bound complex of the vanilloid antagonist capsazepine bound to TRPV1 at 3.8 Å resolution (from ref. [16]).

Phosphoinositide 3-kinase-related kinases

Large proteins (>250 kDa) and large multi-component protein complexes have proved challenging crystallographic targets, and cryo-EM is now being used by structural biologists, including industry groups, to build mechanistic understandings of large protein complexes that are implicated in disease processes. The recent bolus of cryo-EM structures for members of the phosphoinositide 3-kinase-related kinase (PIKK) family demonstrates this well. The family comprises six members that range in molecular mass from the smallest member mTOR (mechanistic target of rapamycin) at nearly 300 kDa to the largest family member DNA-PK (DNA-dependant protein kinase) at ~500 kDa. The proteins can form dimers giving a substantive particle size for cryo-EM imaging and alignment. Additionally, each family member forms a hub around which dynamic multi-component complexes are formed, and cryo-EM is allowing this detailed mechanistic biology to be elucidated. A domain organisation is conserved between family members, an N-terminal α -helical solenoid, a central unit termed the FAT domain and the C-terminal kinase domain. In the past 2 years, an outpouring of cryo-EM structures, at resolutions in the 5–3 Å range, have been reported for the family members mTOR, ATM, ATR, DNA-PK and TRA1/TRRAP (for review, see ref. [22]). The mTOR–Lst8 complex [23] described loosely conserved structural elements across the divergent family, a large N-terminal HEAT repeat containing solenoid (1300 residues in the mTOR case) followed by so-called spiral and bridge domains linking to a more highly conserved C-terminal architecture containing the kinase domain, termed the FATKIN. Additional family member structures rapidly followed, a novel activation mechanism has been postulated for ATM based on two observed conformations of the enzyme [24], while a complex of the close family member ATR with its binding partner ATRIP has been reported at 4.7 Å resolution [25]. Crystallographic and cryo-EM structures have been resolved for DNA-PK in various states [26–28] (Figure 4), the crystal structure at 4.3 Å resolution details the complex of DNA-PK heterodimer with ku70/80 [26], while a cryo-EM holoenzyme structure in complex with ku70/80 and 35-base-pair DNA oligonucleotide at 6.6 Å resolution [28] has further informed our mechanistic understanding. Inhibitors of the PIKK family of enzymes are advancing in the clinic, and DNA-PK, ATM and ATR all play important roles in genomic stability, each initiating diverse DNA damage repair pathways and inhibitors for all three are under investigation in oncology settings. Meanwhile, mTOR inhibitors such as rapamycin itself have long been of interest for their modulation of cellular metabolism, growth and proliferation. No small-molecule inhibitor complex structures have been reported to date; however, as the resolution of the cryo-EM structures improves, these drug-bound PIKK complexes will emerge. The recent 3.0 Å resolution structure of mTORC1, an 1-MDa complex of mTOR and the binding partners RAPTOR and mLst8, and the 3.4 Å structure of mTORC1 bound to the small GTPase RHEB [29] highlight the impact that cryo-EM is having and point to a future in which a firm mechanistic and structural understanding of this diverse family underpins industry discovery programmes.

Mode of action understanding in biological systems

To deliver strong pharmacology and tolerable safety, many successful drugs target a disease relevant protein with a distinct mechanism. Understanding the molecular mode of action (MOA) of drug molecules has therefore become an important part of drug discovery programmes, especially if chemical starting points have an unusual MOA or are from a phenotypic origin, with an undefined molecular target.

Targeting protein–protein interactions by small molecules is often considered highly challenging, but many protein complexes are dynamic, and pharmacological modulation can be achieved not only by PPI inhibition but also through stabilisation of the complex. Two recent examples of stabilising inactive and active complexes of p97 [30] and eIF2B [31,32], respectively, illustrate the increasing power of cryo-EM in revealing novel opportunities for drug interaction with large multiprotein complexes.

The prevalence of oncogenic mutations in p97, an enzyme critical for protein homeostasis, makes it an attractive target for anticancer therapies. Studies of full-length p97 by X-ray crystallography at medium resolution (3.5–4.7 Å) reveal that the AAA+ ATPase forms a donut-like hexamer, with a double-ring core formed by the stacking of the homologous D1 and D2 ATPase domains. In the presence of ATP or stable ATP analogues, extensive protein motion is evident and this conformational heterogeneity has proved problematic for crystallography.

As a single-molecule method, cryo-EM has been able to overcome these difficulties [30]. The single ADP-bound state and the coexistence of three p97 ATPyS-bound conformers have all been resolved at atomic resolution (2.4–3.3 Å), enabling the structural dynamics of the catalytic cycle to be visualised for the first time. The binding of an

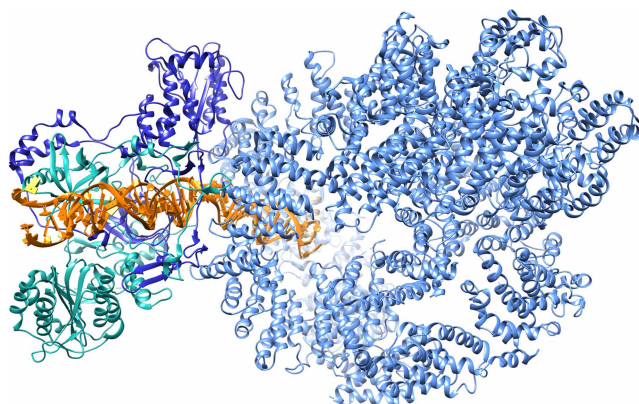


Figure 4. Cryo-EM structure of human DNA-PK holoenzyme.

A 650 kDa 1 : 1 : 1 : 1 complex of DNA-PK, KU70, KU80 and DNA duplex (PDB 5Y3R, [26]).

allosteric small-molecule inhibitor (UPCD30245) could also be clearly visualised by cryo-EM at 2.3 Å (PDB: 5FTJ) (Figure 5). Sandwiched at the interface between two ATPase domains, this compound locks the hexameric complex in a non-functional state preventing the movements required for ATP hydrolysis.

The integrated stress response (ISR) is a conserved translational and transcriptional mechanism that protects cells under assault from viral, UV and other challenges, and affects metabolism, memory and immunity. Regulation of the ISR converges on the phosphorylation of the translation initiation factor eIF2 α , which converts it from a substrate to a competitive inhibitor of its dedicated guanine nucleotide exchange factor, eIF2B, inhibiting translation. In neurological conditions such as brain trauma, the ISR can become dysregulated and starve cells of the protein synthesis necessary to allow repair and return to normal function.

In 2013, Walter [33] and colleagues ran a cellular screen to identify compounds that inhibited EIF2 α activation and found a small-molecule ISR inhibitor, ISRIB, that had nanomolar cellular activity and was remarkably able to protect rodents from neurodegeneration and correct cognitive deficits after brain injury.

Cryo-EM has recently revealed the structural basis of this compound's MOA [31,32]. The rate-determining step in assembling the fully active and decameric eIF2B involves the formation of a dimer of the tetrameric $\alpha\beta\gamma\delta$ subcomplexes. This is the step enhanced by ISRIB, which binds at the interface between the β and δ regulatory subunits and bridges the symmetrical dimer. The propeller-shaped ISRIB sits deep inside the protein and acts as a molecular glue holding the eIF2B complex together to increase its activity thereby counteracting the effect of eIF2 α phosphorylation.

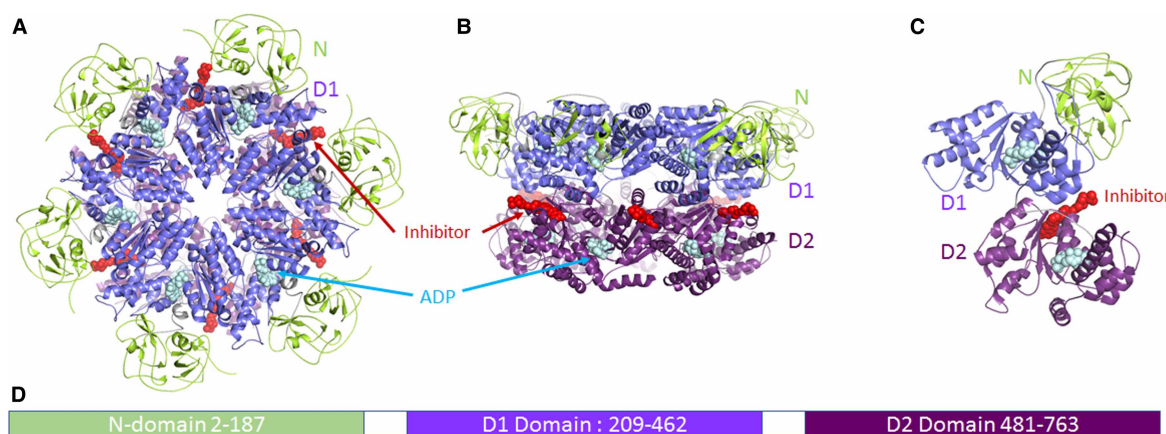


Figure 5. Hexameric p97 cryo-EM structure.

(A) 2.3 Å Hexameric p97 cryo-EM structure (PDB: 5FTJ). (B) Alternate orientations showing ADP (cyan), inhibitor UPDC30245 (red) bound. (C) p97 protomer taken from hexameric structure. (D) Domain architecture of p97 protein.

These rare examples of cryo-EM being able to uncover the atomic details of novel modes of drug action open up the promise of a future where complex biological machinery may be captured in multiple native conformations and visualised with small molecules that perturb or trap distinct states that reveal the most tractable point of pharmacological intervention.

Even in the absence of bound small molecules, cryo-EM can still reveal biologically insightful states, as shown by an increasing number of structures of difficult pharmaceutical targets.

Insulin receptor is a well-studied target for diabetes. Monomeric insulin binding to the ectodomain (ECD) homodimer is characterised by complex binding behaviour best explained by a model in which each receptor monomer has two distinct hormone-binding sites (S1 and S2). The hormone is proposed to bind initially with low affinity to S1 and then cross-link to interact at the second site (S2), resulting in a high-affinity complex that triggers auto-phosphorylation of the intracellular kinase domain and downstream signalling. Crystallographic structures of S1 fragments of the ECD in the presence and absence of insulin have been determined revealing details of the initial complex, but the nature of the signalling complex and the degree of conformational change required for activation were still not understood. A cryo-EM structure, at 4.3 Å resolution [34], for the first time revealed how insulin engages simultaneously S1 and S2. A large conformational change appears critical to access the second site on the first fibronectin type III domain of the ECD and also suggests a mechanism of signal transduction that may provide opportunities for drug design.

Neurodegenerative diseases, such as Alzheimer's disease (AD) and Pick's disease (PiD), are characterised by the presence of abnormally abundant amyloid fibrils of the microtubule-associated protein Tau in brain tissue. The histological appearance of these tau tangles are distinct among these different tauopathies, but until recently the molecular basis of these differences were unknown. Cryo-EM of tau aggregates purified from the brain of AD and PiD patients [35,36] has revealed how the same protein can fold and self-assemble to create these morphologically different forms.

In AD, two types of filaments (paired helical PHFs and straight SFs) are observed. Characterisation by cryo-EM shows that the core of both consists of an identical C-shaped core tau protofilament. Assembly of this subunit across different interfaces generates the different filaments in a manner that allows all six tau isoforms to be included, consistent with the known isoform composition within AD filaments [36].

In PiD, two different tau filaments (narrow NPFs and wide WPFs) are seen. However, the protofilament core is markedly different from that found in AD, being an elongated J-shape. NPFs comprise a single protofilament, while WPFs resemble a pair of NPFs. The structure also explains why Pick body filaments contain only the 3R subset of isoforms. These structures of the core elements of Tau fibrils were enabled by advances in helical reconstruction and identify distinct stretches of amino acids that form the aggregation interface in these diseases. This may permit the targeting of specific peptide sequences for tauopathy inhibitor design and enable the development of disease relevant *in vitro* Tau aggregation assays.

Fab/antigen complexes or Fab enabled structures

Fabs decorating antigens have been a longstanding approach in cryo-EM to identify locations of protein in multi-component complexes, and it has been suggested that they could help with single-particle cryo-EM [37]. With the advent of improved methods for cryo-EM, the utility of Fabs has grown into providing high-resolution structure information on the epitopes and to enable structures to be determined in the first place, by adding mass to relatively small molecules.

In the PDB, there are now 115 structures of complexes containing one or more Fabs. Many are low resolution, but an appreciable number (about one-quarter) are at a high enough resolution to be able to allow modelling of the epitope interface with reasonable confidence (the threshold we suggest for this kind of analysis is 4.2 Å for cryo-EM maps). The vast majority of the higher resolution structures have been published in 2017 and 2018, showing an improvement in samples, data collection and data analysis over previous years.

Other approaches to determining the epitope include HDX [38] coupled with additional biophysical measurements to aid narrowing down the interaction site. One of the most powerful tools for modelling the unknown interaction site is to have high-resolution crystal structures of the components. An example of this is the use of a structure of a Fab targeting chikungunya virus [39]. The Fab structures were determined independently and then fit into a poor cryo-EM map (5.3 Å) of Fab-decorated virus-like particle. By combining the high-resolution information from the X-ray structure and other mutagenesis data, a model for the structure was possible and a hypothesis for the MOA for the antibodies was proposed.

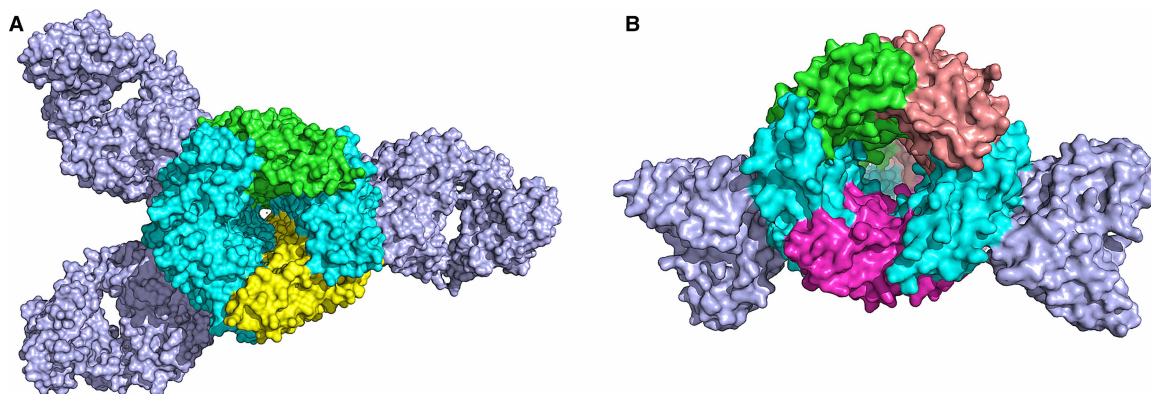


Figure 6. Fab-assisted cryo-EM resolves heterogeneity.

(A) Nicotinic receptor subunit assembly. Fabs (in darker blue) binding to only one subunit type (the b2 subunit in cyan) allow alignment of the particles within a structure that has structurally similar pentamer subunits. (B) The GABAA receptor, a hetero-pentameric structure, shown with two single chain Fvs.

The structure of human-specific 5D3 antibody (Fab) to inhibitor-bound ABCG2 (a drug transporter) was enabled by the addition of the Fabs, to increase the mass by 100 kDa (two Fabs bound per transporter). The resolution of the structure was 3.1 Å, which allowed *de novo* building of the amino acids into the density, and allowed the location and binding orientation of a small-molecule compound to be determined.

Another recent structure in which Fabs aided the structure determination by breaking symmetry in a hetero-pentameric structure [40], and Fabs only bound to one of the subunit types. This allowed alignment of the particles which otherwise would have been difficult or impossible due to the structural similarity between the pentamer subunits (Figure 6A). The same group reported the structure of the GABA_A (γ-aminobutyric acid A) receptor [41], using similar methods of labelling some subunits of a hetero-pentameric receptor (Figure 6B), at a resolution sufficient to detect the binding location of the GABA molecule.

For low-resolution structures (e.g. in the 4–7 Å range), the combination of biophysical methods coupled with X-ray structural information if available and careful modelling is relevant for defining epitopes useful for intellectual property definitions. Where higher resolution structures are attainable, epitope mapping becomes more robust, and Fab enabled structures have been shown to yield structures where otherwise the structure determination would have been problematic or impossible. Alignment of the particles, a key step for averaging, is easier for larger particles, and thus, the prospect for attaining high-resolution information is greater.

Advantages and challenges for drug discovery

In cryo-EM, a small volume of the sample, normally two or three microlitres, is applied to a copper, nickel or carbon grid coated with a support layer (often carbon or gold), and then the vast majority of the protein is removed by blotting with filter paper, to leave a single layer of particles hopefully in random orientations. To prevent the sample drying out in the vacuum of the microscope, the sample is frozen rapidly enough to prevent the formation of ice crystals. The grid is then placed into the microscope, kept at cryogenic temperature, illuminated by the beam of electrons and projections collected on a detector. The electrons have the potential to induce radiation damage and movement in biological specimens, so the electron dose applied must be minimised, resulting in a low signal to noise. Many images are then collected so as to permit projections of the particles to be taken in all directions. The first steps of data processing are to identify the particles in each image (particle picking) and to group them according to their similarity (alignment of particles) to allow averaged projections with improved signal to noise. Challenges for cryo-EM sample preparation include ensuring that the protein molecules are distributed in the vitreous ice and not aggregated at the edge of the holes or at the air–water interface. Finding experimental conditions to achieve this end involves systematic variation of conditions, including pH, additives and grid surface among other variables, and is an iterative process.

Table 1 Protein target, molecular mass, example small-molecule molecular mass of binder, disease indication

Protein	Molecular mass	Small molecule; molecular mass	Disease area	Reference
Leishmania ribosome	1.6 MDa	616	Parasite/infection	[6]
Glpr1R complex	161 kDa	GLP1; 3.3 K	Type 2 diabetes, obesity	[9]
Adenosine 2A receptor	144 kDa	Carboxamido adenosine; 308	Cardio and immune disease	[11]
Adenosine 1 receptor	130 kDa	Adenosine; 267	Ischaemia–reperfusion injury, neuropathic pain	[12]
5HT1B	112 kDa	Donitriptan; 404	Behaviour, migraine	[13]
Mu-opioid receptor	154 kDa	DAMGO; 514	Analgesia	[14]
TRPV1 channel	318 kDa	Resiniferatoxin; 628 Capsazepine; 377	Analgesia	[18]
TRPC6 channel	293 kDa	Inhibitor BTDM; 340	Renal disease, calcium regulation	[21]
DNA-PK	610 kDa	–	Oncology	[28]
p97	650 kDa	UPCD30245; 464	Oncology	[30]
EIF2B transcription factor	545 kDa	Inhibitor; 451	Cognition	[31]
Insulin receptor	221 kDa	–	Diabetes	[34]
Tau	79 kDa (monomer)	–	Neurodegenerative disease	[35,36]

While determining the structure of a macromolecular (individual or in complex) by X-ray crystallography or cryo-EM requires purified protein, in the case of cryo-EM it may be possible to determine the structure using just a few microlitres of a relatively heterogeneous sample. This offers the opportunity to study proteins isolated directly from their native environment, rather than embarking upon generation of affinity tagged proteins expressed in a recombinant system. Any heterogeneity can (in theory) be separated at the cryo-EM data processing stage and can give rise to structures of multiple conformations of a protein, more representative of the protein in solution; the conformational landscape accessible in a crystal lattice is in the best case often greatly reduced and in the worst case, not representative of the conformation of the protein in solution.

An obvious disadvantage of structure determination using X-rays is the absolute requirement for a suitable crystal. When working with a new protein, it is not possible to determine *a priori* what the successful crystallisation conditions will be. However, the robotisation and miniaturisation of protein crystallisation, along with the imaging of the resulting crystallisation trays, and the semi-automated crystal mounting, alignment and data collection allows thousands of conditions and dozens of crystals to be screened in just hours using a single protein sample. If conditions cannot be found, the protein may be engineered to promote crystallisation, for example by deleting mobile regions. This may not be required for cryo-EM structure determination where such conformational heterogeneity will not prevent data from being collected on the protein, but the resulting map will have reduced resolution in these mobile regions. Cryo-EM also has the advantage of, in theory, allowing structures to be solved under different conditions which crystallisation may not permit, e.g. determining the structure at pH values which crystals may not either be formed at or tolerate transfer to.

In contrast, in cryo-EM, the first grid made with the sample may allow the structure to be determined. However, the first grid may also reveal that the protein has aggregated or fallen apart, before or during the process of being applied to the grid and frozen, that insufficient or too much protein has been applied to the grid, or that the vitreous ice is too thin or too thick to permit high-quality images to be collected. In these cases, the systematic variation of conditions and the screening of the resulting grids remain a low throughput and labour intensive process.

This is an area of current development for many cryo-EM groups which will improve reproducibility in the grid-generation process. Once suitable grids have been generated, the recent advances in microscopes, detectors, computers and image processing algorithms may result in structures with near-atomic resolution [42]. However, the signal to noise in a cryo-EM experiment is miniscule, so care must be taken not to over interpret data and maps [43] as validation tools for cryo-EM maps and models become more firmly established [44].

Anticipated technological improvements that will establish cryo-EM in drug discovery

To make cryo-EM a technology that would be embraced by industry more readily, three key areas need to be addressed: (a) ease of making samples and sample tracking, (b) the time it takes to collect and process a data set and (c) cost. Time and cost are linked.

Some key aspects of cryo-EM methodologies and instrumentation improvements are active areas of research to enable future use of cryo-EM in drug development. These include better specimen supports [45] and improved alternative methods for making grids [46]. Better direct electron detectors [47] with back-thinning, electron counting to enhance detective quantum efficiency and a faster read-out rate can increase throughput and data collection times. The routine implementation and use of a phase plate does increase contrast for small proteins <80 kDa [48], and many of the data sets we are collecting already use a phase plate. From a software point of view, on-the-fly processing of images/movies as they are recorded will enable real-time assessment of the quality of the data, to make sure only the best data are collected. These developments will ultimately enhance the structural resolution of cryo-EM, the range of specimens that could be structurally characterised and thus the applicability of cryo-EM for drug development.

Conclusions

Cryo-EM is a nascent technology in the drug discovery industry, stemming from substantial advances in detector technology, microscopes and data processing. Just as fast 2D electronic X-ray detectors and crystal sample changers made high-throughput crystallography practical, the advent of fast multi-frame electron detectors has made collection of high-resolution information from electron microscopes possible. The improvements in the microscopes means that samples could remain in the microscope for days instead of hours, permitting more data to be collected from each sample. The recent adoption of GPU-enabled computers to perform the image processing tasks in much shorter timeframes makes the sample-to-structure cycle more suited to address drug discovery questions. Further improvements in sample preparation coupled with rapid identification of suitable samples mean that it is highly likely that cryo-EM will become a frequently used tool at initial stages of drug discovery, to complement X-ray crystallography and NMR methods.

Abbreviations

AD, Alzheimer's disease; CADD, computer aided drug design; cryo-EM, cryo-electron microscopy; DNA-PK, DNA-dependent protein kinase; ECD, extracellular domain; GABA, γ -aminobutyric acid; ISR, integrated stress response; GLP1R, Glp-1 receptor; GPU, graphics processing unit; MOA, mode of action; mTOR, mechanistic target of rapamycin; PiD, Pick's disease; PIKK, phosphoinositide 3-kinase-related kinase; TRP, transient receptor potential.

Funding

This work was supported by the respective Pharmaceutical companies.

Acknowledgements

We thank Kasim Sader, Rishi Matadeen and Pablo Castro Hartmann from ThermoFisher for providing practical help enabling the consortium members to make efficient use of the Krios microscopes and Raymond Schrijver from ThermoFisher for enabling discussions on how to best meet pharmaceutical company needs in drug discovery using the new electron microscope instruments. We acknowledge the help from various cryo-EM groups at the MRC LMB in Cambridge in helping us both technically and with computational problems. We thank the members of our groups for stimulating discussions and advice.

Competing Interests

The Authors declare that there are no competing interests associated with the manuscript.

References

- 1 Renaud, J.-P., Chari, A., Ciferri, C., Liu, W.-t., Rémy, H.-W., Stark, H. et al. (2018) Cryo-EM in drug discovery: achievements, limitations and prospects. *Nat. Rev. Drug Discov.* **17**, 471–492 <https://doi.org/10.1038/nrd.2018.77>
- 2 Scheres, S.H.W. (2012) A Bayesian view on cryo-EM structure determination. *J. Mol. Biol.* **415**, 406–418 <https://doi.org/10.1016/j.jmb.2011.11.010>

- 3 Bartesaghi, A., Merk, A., Banerjee, S., Matthies, D., Wu, X., Milne, J.L. et al. (2015) 2.2 Å resolution cryo-EM structure of beta-galactosidase in complex with a cell-permeant inhibitor. *Nature* **348**, 1147–1151 <https://doi.org/10.1126/science.aab1576>
- 4 Kühlbrandt, W. (2014) The resolution revolution. *Science* **343**, 1443–1444 <https://doi.org/10.1126/science.1251652>
- 5 Bartesaghi, A., Aguerrebere, C., Falconieri, V., Banerjee, S., Earl, L.A., Zhu, X. et al. (2018) Atomic resolution cryo-EM structure of β -galactosidase. *Structure* **26**, 848–856.e3 <https://doi.org/10.1016/j.str.2018.04.004>
- 6 Shalev-Benami, M., Zhang, Y., Rozenberg, H., Nobe, Y., Taoka, M., Matzov, D. et al. (2017) Atomic resolution snapshot of Leishmania ribosome inhibition by the aminoglycoside paromomycin. *Nat. Commun.* **8**, 1589 <https://doi.org/10.1038/s41467-017-01664-4>
- 7 Liang, Y.-L., Khoshouei, M., Radjainia, M., Zhang, Y., Glukhova, A., Tarrasch, J. et al. (2017) Phase-plate cryo-EM structure of a class B GPCR-G protein complex. *Nature* **546**, 118–123 <https://doi.org/10.1038/nature22327>
- 8 Pal, K., Melcher, K. and Xu, H.E. (2012) Structure and mechanism for recognition of peptide hormones by class B G-protein-coupled receptors. *Acta Pharmacol. Sin.* **33**, 300–311 <https://doi.org/10.1038/aps.2011.170>
- 9 Zhang, Y., Sun, B., Feng, D., Hu, H., Chu, M., Qu, Q. et al. (2017) Cryo-EM structure of the activated GLP-1 receptor in complex with a G protein. *Nature* **546**, 248–253 <https://doi.org/10.1038/nature22394>
- 10 Liang, Y.-L., Khoshouei, M., Glukhova, A., Furness, S.G.B., Zhao, P., Clydesdale, L. et al. (2018) Phase-plate cryo-EM structure of a biased agonist-bound human GLP-1 receptor-Gs complex. *Nature* **555**, 121–125 <https://doi.org/10.1038/nature25773>
- 11 García-Nafria, J., Lee, Y., Bai, X., Carpenter, B. and Tate, C.G. (2018) Cryo-EM structure of the adenosine A2A receptor coupled to an engineered heterotrimeric G protein. *eLife* **7**, e35946 <https://doi.org/10.7554/eLife.35946>
- 12 Draper-Joyce, C.J., Khoshouei, M., Thal, D.M., Liang, Y.-L., Nguyen, A.T.N., Furness, S.G.B. et al. (2018) Structure of the adenosine-bound human adenosine A₁ receptor-G_i complex. *Nature* **558**, 559–563 <https://doi.org/10.1038/s41586-018-0236-6>
- 13 García-Nafria, J., Nehmé, R., Edwards, P.C. and Tate, C.G. (2018) Cryo-EM structure of the serotonin 5-HT_{1B} receptor coupled to heterotrimeric G_o. *Nature* **558**, 620–623 <https://doi.org/10.1038/s41586-018-0241-9>
- 14 Koehl, A., Hu, H., Maeda, S., Zhang, Y., Qu, Q., Paggi, J.M. et al. (2018) Structure of the μ -opioid receptor-G_i protein complex. *Nature* **558**, 547–552 <https://doi.org/10.1038/s41586-018-0219-7>
- 15 Madej, M.G. and Ziegler, C.M. (2018) Dawning of a new era in TRP channel structural biology by cryo-electron microscopy. *Eur. J. Physiol.* **470**, 213–225 <https://doi.org/10.1007/s00424-018-2107-2>
- 16 Bayburt, T.H. and Sligar, S.G. (2010) Membrane protein assembly into nanodiscs. *FEBS Lett.* **584**, 1721–1727 <https://doi.org/10.1016/j.febslet.2009.10.024>
- 17 Cao, E., Liao, M., Cheng, Y. and Julius, D. (2013) TRPV1 structures in distinct conformations reveal activation mechanisms. *Nature* **504**, 113–118 <https://doi.org/10.1038/nature12823>
- 18 Gao, Y., Cao, E., Julius, D. and Cheng, Y. (2016) TRPV1 structures in nanodiscs reveal mechanisms of ligand and lipid action. *Nature* **534**, 347–351 <https://doi.org/10.1038/nature17964>
- 19 Yang, F., Xiao, X., Cheng, W., Yang, W., Yu, P., Song, Z. et al. (2015) Structural mechanism underlying capsaicin binding and activation of the TRPV1 ion channel. *Nat. Chem. Biol.* **11**, 518–524 <https://doi.org/10.1038/nchembio.1835>
- 20 Paulsen, C.E., Armache, J.-P., Gao, Y., Cheng, Y. and Julius, D. (2015) Structure of the TRPA1 ion channel suggests regulatory mechanisms. *Nature* **520**, 511–517 <https://doi.org/10.1038/nature14367>
- 21 Tang, Q., Guo, W., Zheng, L., Wu, J.-X., Liu, M., Zhou, X. et al. (2018) Structure of the receptor-activated human TRPC6 ion channels. *Cell Res.* **28**, 746–755 <https://doi.org/10.1038/s41422-018-0038-2>
- 22 Imseng, S., Ayllett, C.H.S. and Maier, T. (2018) Architecture and activation of phosphatidylinositol 3-kinase related kinases. *Curr. Opin. Struct. Biol.* **49**, 177–189 <https://doi.org/10.1016/j.sbi.2018.03.010>
- 23 Baretic, D., Berndt, A., Ohashi, Y., Johnson, C.M. and Williams, R.L. (2016) Tor forms a dimer through an N-terminal helical solenoid with a complex topology. *Nat. Commun.* **7**, 11016 <https://doi.org/10.1038/ncomms11016>
- 24 Baretic, D., Pollard, H.K., Fisher, D.I., Johnson, C.M., Santhanam, B., Truman, C.M. et al. (2017) Structures of closed and open conformations of dimeric human ATM. *Sci. Adv.* **3**, e1700933 <https://doi.org/10.1126/sciadv.1700933>
- 25 Rao, Q., Liu, M., Tian, Y., Wu, Z., Hao, Y., Song, L. et al. (2017) Cryo-EM structure of human ATR-ATRIP complex. *Cell Res.* **28**, 143–156 <https://doi.org/10.1038/cr.2017.158>
- 26 Sibanda, B.L., Chirgadze, D.Y., Ascher, D.B. and Blundell, T.L. (2017) DNA-PKcs structure suggests an allosteric mechanism modulating DNA double-strand break repair. *Science* **355**, 520–524 <https://doi.org/10.1126/science.aak9654>
- 27 Yin, X., Liu, M., Tian, Y., Wang, J. and Xu, Y. (2017) Cryo-EM structure of human DNA-PK holoenzyme. *Cell Res.* **27**, 1341–1350 <https://doi.org/10.1038/cr.2017.110>
- 28 Sharif, H., Li, Y., Dong, Y., Dong, L., Wang, W.L., Mao, Y. et al. (2017) Cryo-EM structure of the DNA-PK holoenzyme. *Proc. Natl Acad. Sci. U.S.A.* **114**, 7367–7372 <https://doi.org/10.1073/pnas.1707386114>
- 29 Yang, H., Jiang, X., Li, B., Yang, H.J., Miller, M., Yang, A. et al. (2017) Mechanisms of mTORC1 activation by RHEB and inhibition by PRAS40. *Nature* **552**, 368–373 <https://doi.org/10.1038/nature25023>
- 30 Banerjee, S., Bartesaghi, A., Merk, A., Rao, P., Bulfer, S.L., Yan, Y. et al. (2016) 2.3 Å resolution cryo-EM structure of human p97 and mechanism of allosteric inhibition. *Science* **351**, 871–875 <https://doi.org/10.1126/science.aad7974>
- 31 Zryanova, A.F., Weis, F., Faille, A., Alard, A.A., Crespillo-Casado, A., Sekine, Y. et al. (2018) Binding of ISRIB reveals a regulatory site in the nucleotide exchange factor eIF2B. *Science* **359**, 1533–1536 <https://doi.org/10.1126/science.aar5129>
- 32 Tsai, J.C., Miller-Vedam, L.E., Anand, A.A., Jaishankar, P., Nguyen, H.C., Renslo, A.R. et al. (2018) Structure of the nucleotide exchange factor eIF2B reveals mechanism of memory-enhancing molecule. *Science* **359**, eaag0939 <https://doi.org/10.1126/science.aag0939>
- 33 Sidrauski, C., Acosta-Alvear, D., Khoutorsky, A., Vedantham, P., Hearn, B.R., Li, H. et al. (2013) Pharmacological brake-release of mRNA translation enhances cognitive memory. *eLife* **2**, e00498 <https://doi.org/10.7554/eLife.00498>
- 34 Ward, C.W., Menting, J.G. and Lawrence, M.C. (2013) The insulin receptor changes conformation in unforeseen ways on ligand binding: sharpening the picture of insulin receptor activation. *BioEssays* **35**, 945–954 <https://doi.org/10.1002/bies.201300065>

- 35 Falcon, B., Zhang, W., Schweighauser, M., Murzin, A.G., Vidal, R., Garringer, H.J. et al. (2018) Tau filaments from multiple cases of sporadic and inherited Alzheimer's disease adopt a common fold. *Acta Neuropathol.* **136**, 699–708 <https://doi.org/10.1007/s00401-018-1914-z>
- 36 Fitzpatrick, A.W.P., Falcon, B., He, S., Murzin, A.G., Murshudov, G., Garringer, H.J. et al. (2017) Cryo-EM structures of tau filaments from Alzheimer's disease. *Nature* **547**, 185–190 <https://doi.org/10.1038/nature23002>
- 37 Wu, S., Avila-Sakar, A., Kim, J., Booth, D.S., Greenberg, C.H., Rossi, A. et al. (2012) Fabs enable single particle cryoEM studies of small proteins. *Structure* **20**, 582–592 <https://doi.org/10.1016/j.str.2012.02.017>
- 38 Oganessian, I., Lento, C. and Wilson, D.J. (2018) Contemporary hydrogen deuterium exchange mass spectrometry. *Methods* **144**, 27–42 <https://doi.org/10.1016/j.ymeth.2018.04.023>
- 39 Long, F., Fong, R.H., Austin, S.K., Chen, Z., Klose, T., Fokine, A. et al. (2015) Cryo-EM structures elucidate neutralizing mechanisms of anti-chikungunya human monoclonal antibodies with therapeutic activity. *Proc. Natl Acad. Sci. U.S.A.* **112**, 13898–13903 <https://doi.org/10.1073/pnas.1515558112>
- 40 Walsh, R.M., Jr., Roh, S.-H., Gharpure, A., Morales-Perez, C.L., Teng, J. and Hibbs, R.E. (2018) Structural principles of distinct assemblies of the human $\alpha 4\beta 2$ nicotinic receptor. *Nature* **557**, 261–265 <https://doi.org/10.1038/s41586-018-0081-7>
- 41 Zhu, S., Noviello, C.M., Teng, J., Walsh, R.M. Jr, Jeong Joo Kim, J.J. and Hibbs, R.E. (2018) Structure of a human synaptic GABA_A receptor. *Nature* **559**, 67–72 <https://doi.org/10.1038/s41586-018-0255-3>
- 42 Bai, X.-c., McMullan, G. and Scheres, S.H.W. (2015) How cryo-EM is revolutionizing structural biology. *Trends Biochem. Sci.* **40**, 49–57 <https://doi.org/10.1016/j.tibs.2014.10.005>
- 43 Henderson, R. (2013) Avoiding the pitfalls of single particle cryo-electron microscopy: Einstein from noise. *Proc. Natl Acad. Sci. U.S.A.* **110**, 18037–18041 <https://doi.org/10.1073/pnas.1314449110>
- 44 Afonine, P.V., Klaholz, B.P., Moriarty, N.W., Poon, B.K., Sobolev, O.V., Terwilliger, T.C. et al. (2018) New tools for the analysis and validation of cryo-EM maps and atomic models. *bioRxiv* <https://doi.org/10.1101/279844>
- 45 Russo, C.J. and Passmore, L.A. (2014) Ultrastable gold substrates for electron cryomicroscopy. *Science* **346**, 1377–1380 <https://doi.org/10.1126/science.1259530>
- 46 Jain, T., Sheehan, P., Crum, J., Carragher, B. and Potter, C.S. (2012) Spotiton: a prototype for an integrated inkjet dispense and vitrification system for cryo-TEM. *J. Struct. Biol.* **179**, 68–75 <https://doi.org/10.1016/j.jsb.2012.04.020>
- 47 Kuijper, M., van Hoften, G., Janssen, B., Geurink, R., De Carlo, S., Vos, M. et al. (2015) FEI's direct electron detector developments: embarking on a revolution in cryo-TEM. *J. Struct. Biol.* **192**, 179–187 <https://doi.org/10.1016/j.jsb.2015.09.014>
- 48 Khoshouei, M., Radjainia, M., Baumeister, W. and Danev, R. (2017) Cryo-EM structure of haemoglobin at 3.2 Å determined with the Volta phase plate. *Nat. Commun.* **8**, 16099 <https://doi.org/10.1038/ncomms16099>